Ecological Modelling 478 (2023) 110302

Contents lists available at ScienceDirect

Ecological Modelling

journal homepage: www.elsevier.com/locate/ecolmodel

A dynamic thermal model for predicting internal temperature of tree cavities and nest boxes

Taylor B. Velander [a,b,*], Michael J. Joyce [b], Angela M. Kujawa [c,1], Robert L. Sanders [c,2], Paul W. Keenlance [d], Ron A. Moen [b,e]

[a] Integrated Biosciences Graduate Program, University of Minnesota Duluth, 1035 Kirby Drive, Duluth, MN 55812, United States
[b] Natural Resources Research Institute, University of Minnesota Duluth, 5013 Miller Trunk Hwy, Duluth, MN 55811, United States
[c] Natural Resources Department, Little River Band of Ottawa Indians, 2608 Government Center Drive, Manistee, MI 49660, United States
[d] Biology Department, Grand Valley State University, Allendale, MI 49401, United States
[e] Department of Biology, University of Minnesota Duluth, 1035 Kirby Drive, Duluth, MN 55812, United States

ARTICLE INFO

Keywords:
Thermal ecology
Thermoregulation
Microclimate
Heat transfer
American marten
Fisher

1. Introduction

Many mammal and bird species use tree cavities for resting and raising offspring (Moore, 1945; McComb and Noble, 1981b; Isaac et al., 2008; Cockle et al., 2011; Maziarz et al., 2017; van der Hoek et al., 2017). Tree cavities protect inhabitants from predators and harsh weather and provide favorable microclimates. Energetic costs of thermoregulation during periods of extreme ambient temperatures are reduced when birds and mammals use tree cavities (Kendeigh, 1961; Du Plessis et al., 1994; Zalewski, 1997; Sedgeley, 2001; Joyce, 2013; Matthews et al., 2019). Further, favorable thermal conditions in tree cavities may reduce the energetic costs of reproduction, enhance egg viability, and increase offspring growth rate (Wiebe and Swift, 2001; Ardia et al., 2006; Clement and Castleberry, 2013).

Temperatures within tree cavities and other microhabitats are influenced by local weather conditions, site characteristics, and the thermal and structural properties of the microhabitat that modulate heat and mass transfer processes between the microhabitat and its environment (Kearney and Porter, 2017). For example, the tree canopy can partially block solar insolation and decrease local ambient temperatures in a forest (Leuzinger et al., 2010; Berry et al., 2013; De Frenne et al., 2019). Other site characteristics such as the slope and orientation of the terrain at the tree cavity site also affect site temperature (Suggitt et al., 2011; Méndez-Toribio et al., 2016). Characteristics of the cavity, such as orientation of entrance holes, size of entrance holes, chamber volume, chamber diameter, wall thickness, internal surface area, and the specific heat capacity of the wood surrounding the cavity affect internal cavity temperatures (MacLean, 1941; Sedgeley, 2001; Ardia et al., 2006; Paclík and Weidinger, 2007; Clement and Castleberry, 2013; Radmanović et al., 2014). For example, temperatures within cavities are more stable and fluctuate less with increasing tree diameter (Coombs et al., 2010). This is partly because increased wood around cavity chambers resists heat flow between the cavity chamber and the external environment. Similarly, temperatures in cavities with many entrance holes or cavities with large entrance holes are likely less stable due to greater air movement into and out of the cavity.

Moisture also plays an important role in microhabitat temperatures when water freezes and thaws. In trees without cavities, for example, internal wood temperature is partially governed by phase changes of water or sap that occur when temperatures reach freeze-thaw (Derby

* Corresponding author at: Natural Resources Research Institute, University of Minnesota Duluth, 5013 Miller Trunk Hwy, Duluth, MN 55811, United States.
E-mail address: velan018@d.umn.edu (T.B. Velander).
[1] Michigan Department of Natural Resources, Wildlife Division, M 33 Atlanta, Michigan 49,709, United States.
[2] Michigan Department of Natural Resources, Wildlife Division, 2468W 24th St. Baldwin, Michigan 49,304, United States.

https://doi.org/10.1016/j.ecolmodel.2023.110302
Received 6 October 2022; Received in revised form 21 January 2023; Accepted 24 January 2023
Available online 1 February 2023

and Gates, 1966; Graf et al., 2015; Charrier et al., 2017; Reid et al., 2020; Zhao et al., 2021), which is the temperature range at which water changes between liquid and solid phases. Freeze-thaw for pure water is 0°C, but freeze-thaw can be slightly warmer or cooler for aqueous solutions such as tree sap (Derby and Gates, 1966; Graf et al., 2015; Reid et al., 2020; Zhao et al., 2021). Graf et al. (2015) describe the fundamental phase change dynamics within trees. Water frozen in a tree undergoes a phase change from a solid state to a liquid state as temperatures in the tree reach freeze-thaw. During this phase change, the latent heat of fusion of ice keeps the wood at temperatures around freeze-thaw even if ambient temperature is above freeze-thaw temperatures. This period of relatively constant temperature around freeze-thaw is called a thermal arrest period, and it does not end until the ice fully thaws. Similarly, during freezing, the latent heat of solidification of liquid water creates a thermal arrest period around freeze-thaw until the water has fully solidified. Latent heat of water is also responsible for thermal arrest periods that occur during the freezing and thawing of moist soil (Kudriavtcev et al., 2016; Zhou et al., 2018; Zhang et al., 2020). Phase change of water is also a key component in the development of the subnivium and is a process that allows the subnivium to maintain a temperature of around 0°C throughout the winter in areas with relatively deep snowpack (Cohen, 1994; Thompson et al., 2018; Kearney, 2020). The effects of thermal arrest periods on tree cavity temperatures has not been documented. However, we expect that thermal arrest periods may occur in cavities due to the prevalence of this phenomenon in solid tree stems and other microhabitats.

Many animals select cavities based on the relative thermal benefit they provide. For example, female fishers (*Pekania pennanti*) (Aubry et al., 2013; Matthews et al., 2019), tree swallows (*Tachycineta bicolor*) (Ardia et al., 2006), and bats (Lausen and Barclay, 2003; Ruczyński, 2006) all change cavity selection to match varying cavity temperatures with their changing biological needs. Having the ability to predict the temperature in tree cavities could improve our mechanistic understanding of the role of cavity characteristics on animal selection and ecology, and provide a biological basis for management decisions. Temperature loggers are often used to make a direct connection between animal response and microhabitat temperature (Vonhof and Barclay, 1997; Wiebe, 2001; Paclík and Weidinger, 2007; Isaac et al., 2008; Coombs et al., 2010; Mersten-Katz et al., 2012; Maziarz et al., 2017; Fawcett et al., 2019). Although accurate, temperature loggers are limited to measuring temperatures of a single cavity, cannot predict historical temperatures, and are limited to measuring temperatures until either the memory is filled or the batteries run low. Consequently, the limitations of temperature loggers increase the cost and effort needed to measure tree cavity temperatures, making it relatively difficult for researchers to effectively sample tree cavity temperatures.

An alternative method is to create a model that can be used to predict historical and future temperatures in cavities as a function of changes in weather conditions, habitat characteristics, and cavity characteristics. A variety of thermal modeling approaches have been used to measure or estimate heat flow and temperatures of systems similar to tree cavities. Complex theoretical heat transfer equations can be used to model a broad range of heat and mass transfer processes (Potter and Andresen, 2002; Westermann et al., 2013; Kearney and Porter, 2017; Reid et al., 2020). This modeling approach, however, often requires many parameters and is computationally intensive. An alternative approach is to use theoretical equations that represent the most important processes of heat and mass transfer (Bolstad et al., 1997). Although this approach is simple, it can be less accurate, resulting in a trade-off between model complexity and model accuracy (Gilad-Bachrach et al., 2003). There are also hybrid modeling approaches, which use a simple theoretical structure as the foundation of the model and obtain empirical estimates of the systems temperature to calibrate or fit the model (Bryant and Shreeve, 2002; Maclean et al., 2017; Singh and Tiwari, 2017; Hietaharju et al., 2018; Cui et al., 2019). The hybrid approach can produce accurate results for systems that are measured, but the hybrid model cannot be extended to other systems without acquiring new empirical temperature measurements for calibration.

There are few studies that predict tree cavity temperatures. Studies that do, however, use data driven approaches that include empirical measurements of tree cavity temperatures as a parameter within the model (Howe et al., 1987; Clement and Castleberry, 2013; Amat-Valero et al., 2014; Güebler et al., 2014). These models cannot be extended to other cavities or different time periods, limiting the scope of their application. They also did not directly predict tree cavity temperatures by accounting for the site-specific abiotic conditions and cavity characteristics that drive the heat and mass transfer of energy between the cavity and external environment. For example, Amat-Valero et al. (2014) used measured cavity temperatures and relative humidity to calculate the apparent, or perceived, temperature in tree cavities. Although the model they developed was useful, it required them to measure tree cavity temperature, which further supports the need for an alternative way to obtain cavity temperature.

In this study we describe a theoretical thermal model that accurately predicts temperature in tree cavities over time. The model requires a relatively small set of measurements for parameterization but has a tractable complexity that captures the main heat and mass transfer processes that drive temperature within the tree cavity. It is also generalizable, allowing researchers to use the model on different tree cavities that experience different ambient temperatures, and vary in physical, thermal, and site characteristics. The model uses ambient temperature and cavity-specific thermal and physical characteristics to predict the temperatures within tree cavities over time. Our objectives were to: 1) define a tree cavity system by identifying the major processes of heat and mass transfer that influence cavity temperatures; 2) describe a thermal model that incorporates the major heat and mass transfer processes to estimate cavity temperatures; and 3) test the model's ability to accurately predict temperatures in tree cavities. We also tested the model's ability to predict temperatures in den boxes, which are known to be important alternative microhabitats in areas where natural tree cavities are limited (McComb and Noble, 1981a; Mänd et al., 2005; Lindenmayer et al., 2009; Goldingay et al., 2015; Maziarz et al., 2017).

2. Methods

2.1. Defining the cavity system

Temperature within a cavity chamber varies over time as energy is constantly exchanged between the environment and the cavity. Thermal equilibrium is unlikely to be reached because of daily cycles in ambient temperature. Energy flow equations can account for a cavity's transient flow of energy by using partial derivatives (Potter and Andresen, 2002; Reid et al., 2020). An alternative approach is to treat cavity systems as a lumped capacitance reservoir of heat, which simplifies transient heat analyses by removing the space variable and allowing temperature to be predicted as a function of time, and assume radiation and convection are negligible (Hudson and Underwood, 1982; Kossak and Stadler, 2015; Hietaharju et al., 2018). Using these simplifying assumptions, we treated a tree cavity system as a lumped capacitance reservoir of heat with two main processes of heat and mass transfer occurring (Fig. 1): (1) conductive heat (Q_{cond}) transferred between ambient air and the cavity system; and (2) the displacement of air and the associated heat (Q_{hole}) through one or more entrance holes.

2.2. Cavity model description

The model we describe uses a framework of heat and mass transfer equations similar to the equations described by Kossak and Stadler (2015) and Hietaharju et al. (2018). We modified the use of these equations for tree cavities and den boxes that would be used by animals.

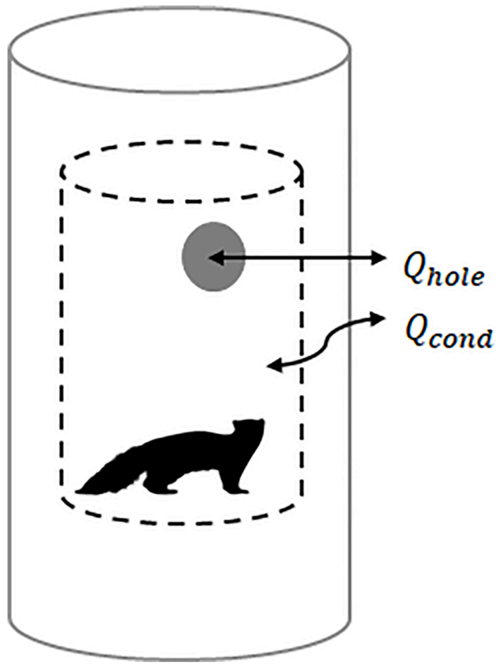

Fig. 1. Schematic of the primary heat and mass transfer processes in a tree cavity system. Q_{cond} is the conductive heat transferred between ambient air and the cavity system, and Q_{hole} is the mass transfer of air through an entrance hole (s). Both Q_{cond} and Q_{hole} are expressed in joules (J). The dashed line represents the cavity chamber.

2.2.1. Energy change equations

The energy transfer rate (Watts) through any system is equal to the sum of the energy transfer rates in and out of the system. Eq. (1) describes the energy transfer rate through a cavity system based on Q_{cond} and Q_{hole}:

$$\frac{dQ_{cavity}}{dt} = \frac{dQ_{cond}}{dt} + \frac{dQ_{hole}}{dt} \tag{1}$$

where $\frac{dQ_{cavity}}{dt}$ is the cumulative energy transfer rate through the cavity system, $\frac{dQ_{cond}}{dt}$ is the conductive heat transfer rate between the ambient air and the cavity system, and $\frac{dQ_{hole}}{dt}$ is the mass transfer rate of air moving through the entrance hole(s) of the cavity system.

Heat transfer between the ambient air and the inside cavity chamber is resisted by all sides of the cavity chamber except the entrance hole(s). A side is comprised of one or more layers of material (i.e., wood, bark, insulation). The conductive heat transfer through a single side of a cavity can be expressed as the product of the overall heat transfer coefficient of the side, the outer surface area of the side, and the difference between the ambient temperature and the temperature of air in the cavity:

$$\frac{dQ_{cond}}{dt} = U_s A_s [T_a - T_{in}] \tag{2}$$

where U_s is the overall heat transfer coefficient of a side (W/m^{2}K) and is calculated using the thermal conductivity (W/mK) and thickness (m) of each layer of the side (Bergman et al., 2011), A_s is the outer surface area of the side (m^2), T_{in} is the internal cavity temperature (K), and T_a is the ambient air temperature outside the cavity (K). To account for conductive heat transfer through all sides of a cavity chamber, the heat loss coefficient U_sA_s (W/K) can be calculated as the sum of the products of the overall heat transfer coefficients and surface areas of each side of the cavity (Kossak and Stadler, 2015):

$$U_s A_s = \sum_{i=1}^{n} U_{s(i)} A_{s(i)} \tag{3}$$

where $U_{s(i)}$ is the overall heat transfer coefficient of side i (W/m^{2}K), and $A_{W(i)}$ is the outer surface area of side i (m^2).

The mass transfer rate of air moving through the entrance hole(s) of a cavity system is calculated from volumetric air flow into the cavity through the entrance hole(s), the density of the ambient air, the isobaric specific heat capacity of the ambient air, and the temperature difference between the internal air volume and the ambient air (Kossak and Stadler, 2015):

$$\frac{dQ_{hole}}{dt} = \left(\dot{V}_{air} \times \rho_{air_a} \times C_{p,air_a}\right)[T_a - T_{in}] \tag{4}$$

where V_{air} is the volumetric air flow into the cavity through entrance hole(s) (m^3/s), and is estimated as the product of the surface area (m^2) of the entrance hole and the speed (m/s) at which air is moving through. ρ_{air_a} is the density of the ambient air (kg/m^3), and C_{p,air_a} is the isobaric specific heat capacity of the ambient air (J/kgK).

In a cavity system, heat and mass transfer processes act on two separate heat sinks (Kossak and Stadler, 2015): the air volume in the cavity chamber, and the materials such as wood, bark, bedding material, or insulation that make up the cavity structure (Fig. 1). We accounted for heat and mass transfer through each of these sinks by re-expressing Eq. (1) as the sum of the energy transfer rate through the air volume and the energy transfer rate through the material volume:

$$\frac{dQ_{air}}{dt} + \frac{dQ_m}{dt} = \frac{dQ_{cond}}{dt} + \frac{dQ_{hole}}{dt} \tag{5}$$

where $\frac{dQ_{air}}{dt}$ is the energy transfer rate through the air volume in the system and $\frac{dQ_m}{dt}$ is the energy transfer rate through the material volume.

2.2.2. Modified energy change equations

Eqs. (1-5) predict energy change of the cavity system over time. We can predict temperature change over time using the heat capacity (J/K) of the air and the heat capacity of the materials (Kossak and Stadler, 2015; Hietaharju et al., 2018). We expressed the energy change (J) of the air volume in the system as the product of the heat capacity of the air and the change in air temperature in the cavity chamber, with heat capacity of air being equivalent to the product of the volume, density, and isobaric specific heat capacity of the air mass:

$$dQ_{air} = C_{air} \times dT_{in} = \left(V_{air} \times \rho_{air_{in}} \times C_{p,air_{in}}\right) \times dT_{in} \tag{6}$$

where C_{air} is the heat capacity of the air volume in the cavity chamber (J/K), dT_{in} is the change in air temperature in the cavity chamber (K), V_{air} is the volume of the air in the cavity chamber (m^3), $\rho_{air_{in}}$ is the density of air in the cavity chamber (kg/m^3), and $C_{p,air_{in}}$ is the isobaric specific heat capacity of air in the cavity chamber (J/kgK).

The energy change through a material volume is the product of the heat capacity of the material volume and the change in air temperature inside the cavity:

$$dQ_m = C_m \times dT_{in} \tag{7}$$

where C_m is the heat capacity of the material volume (J/K). The cavity system, however, can be composed of several materials, with each material having its own heat capacity value. Because we are treating the cavity as a lumped capacitance system, the heat capacity of the material volume (C_m) is calculated as the sum of the heat capacities of all materials in the cavity system, with the heat capacity of material i equal to the product of its specific heat capacity, its volume, and its density:

$$C_m = \sum_{i=1}^{n} C_{m(i)} = \sum_{i=1}^{n} C_i \times V_i \times \rho_i \tag{8}$$

where $C_{m(i)}$ is the heat capacity of material i (J/K), C_i is the specific heat capacity of material i (J/kgK), V_i is the volume of material i (m^3), and ρ_i

is the density of material *i* (kg/m^3). Eq. (5) can now be re-evaluated as:

$$\left(C_m \times \frac{dT_{in}}{dt}\right) + \left(C_{air} \times \frac{dT_{in}}{dt}\right) = \frac{dQ_{cond}}{dt} + \frac{dQ_{hole}}{dt} \tag{9}$$

Eq. (9) can be expressed as a first order differential equation, where air temperature in the cavity chamber at time *t* can be predicted using values of T_{in} and T_a at the previous time step $(t-1)$:

$$T_{in(t)} = T_{in(t-1)} + \frac{\Delta t}{\left(C_m + C_{air(t-1)}\right)}\left[\left(U_s A_s\left[T_{a(t-1)} - T_{in(t-1)}\right]\right) + \left(\left(\dot{V}_{air} \times \rho_{air_a(t-1)} \times C_{\rho,air_a(t-1)}\right)\left[T_{a(t-1)} - T_{in(t-1)}\right]\right)\right] \tag{10}$$

$T_{in(t)}$ is the predicted internal temperature (K) at the current time step (t), $T_{in(t-1)}$ is the estimated internal temperature at the previous time step $(t-1)$, $T_{a(t-1)}$ is the ambient temperature (K) at the previous time step $(t-1)$, and Δt is the time interval (seconds) between t and $t-1$. Because the density and isobaric specific heat capacity of air changes with temperature, $C_{air(t-1)}$ is the heat capacity of the air volume in the cavity chamber at $(t-1)$, $\rho_{air_a(t-1)}$ is the density of ambient air (kg/m^3) at $(t-1)$, and $C_{\rho,air_a(t-1)}$ is the isobaric specific heat capacity of ambient air (J/kgK) at $(t-1)$.

2.3. Model evaluation

2.3.1. Study areas

The Superior and Chippewa National Forests, Minnesota USA, are described by Joyce (2013), and Berg et al. (2020). Superior National Forest is in northeastern Minnesota (47.30 °N, 91. 52 °W), and consists of four main forest cover types: mixed coniferous-deciduous forest, lowland conifer, upland conifer, and deciduous forest. The Chippewa National Forest is in north-central Minnesota, near Remer, Minnesota (47.06 °N, 93.91°W), and consists mostly of deciduous forest, with areas of open water, wetlands, regenerating and mixed forests.

The Huron-Manistee National Forest, Michigan USA, was described by Sanders et al. (2017). The study area is in Michigan's northern lower peninsula (44.42 °N, 85.40 °W), and consists of a variety of upland forest types such as mixed-hardwood and second-growth conifer stands.

2.3.2. Field data collection

We collected ambient and cavity temperature data at 22 cavities in the Chippewa and Superior National and 21 cavities in the Huron-Manistee National Forest. The cavities we measured were used by American martens (*Martes americana*) and fishers during previous radiotelemetry studies. We selected a sub-sample from 218 cavities previously identified in Minnesota and 143 cavities previously identified in Michigan (Joyce, 2013; Erb et al., 2015; Sanders et al., 2017). We used a stratified random sampling design to select cavities to sample based on three strata for tree diameter and three strata for cavity hole height above ground. We constrained the final sample to be similar to tree species composition, tree diameter, and status (live or dead) of trees used by martens or fishers. Our final sample included cavities in quaking aspen trees ($N = 12$, *Populus tremuloides*), northern white cedar trees ($N = 6$, *Thuja occidentalis*), red maple trees ($N = 3$, *Acer rubrum*), and a paper birch tree ($N = 1$, *Betula papyrifera*) in Minnesota. We sampled cavities in oak trees ($N = 15$, *Quercus* spp.), bigtooth aspen trees ($N = 2$; *Populus grandidentata*), and sugar maple trees ($N = 4$, *Acer saccharum*) in Michigan. We sampled 29 cavities in live trees and 14 cavities in dead trees. Trees in Minnesota had an average diameter at breast height (DBH) of 43.2 cm (SD = 10.9, range = 26.7–71.9), while trees in Michigan had an average DBH of 57.8 cm (SD = 18.7, range = 36.1–96.5). Average cavity height above the ground in Minnesota was 3.2 m (SD = 1.8, range = 0.6–8.3), while average cavity height above ground in Michigan was 3.3 m (SD = 2.3, range = 0–8.4).

We also tested the model on 27 fisher den boxes (hereafter, artificial cavities) installed in the Chippewa and Superior National Forests. Artificial cavities were made from plywood or a combination of plywood and foam insulation and were used in a fisher habitat improvement study in northern Minnesota (M. Joyce, unpublished data). Artificial cavities were installed 2.5–3 m above ground on live trees.

For natural cavities, we measured each cavity using the entrance hole(s) as the access point. We used a string with washers tied to the end to measure distance to the floor of the cavity, a length of 16-gauge wire to measure the distance to the ceiling of the cavity, a diameter tape to measure the diameter of the bole at cavity entrance height, and a tape measure to measure inside diameter, the thickness of the wood surrounding the inner cavity, and entrance hole height and width. The thickness of the wood surrounding the inner cavity was estimated by taking the difference between the total diameter of the tree cavity and cavity chamber diameter and dividing by two. We used the tree cavity measurements to calculate the volume of the internal cavity space, the volume of wood and bark, the total surface area of the cavity, and the area of the entrance hole. We calculated these values by assuming the entrance hole is the shape of an ellipse, the entire cavity system was a cylinder, the internal cavity space was a cylinder, and that the thickness of wood around the cavity was uniform (Clement and Castleberry, 2013). Conductive heat transfer from the ambient air to the inner cavity space occurs through the ceiling of the cavity chamber, the floor of the cavity chamber, and the wall surrounding the cavity chamber. For calculation purposes we assumed all sides of the cavity had the same thickness and thermal properties. We assumed the bark layer had the same thermal properties as the wood layer. Wood density, specific heat capacity, and thermal conductivity of the cavity wood (Table 1) were estimated from literature values for each tree species (Dunlap, 1912; TenWolde et al., 1988; Hedlund and Johansson, 2000; Repola, 2006). Each cavity varied in its physical and thermal characteristics (Supplementary S1 and S2).

Table 1
Density, specific heat, and thermal conductivity values used for estimating model parameters.

Material	Density (kg/m^3)	Specific Heat Capacity (J/kgK)	Thermal Conductivity (W/mK)
Maple wood (*Acer* spp.)	660	1369	0.18
Aspen wood (*Populus* spp.)	410	1377	0.12
Oak wood (*Quercus* spp.)	720	1361	0.19
Cedar wood (*Thuja* spp.)	385	1357	0.09
Pine plywood (*Pinus* spp.)	580	1369	0.10
Aspen plywood (*Populus* spp.)	580	1369	0.10
Douglas fir plywood (*Pseudotsuga menziesii*)	525	1360	0.12
Extruded polystyrene	33	1428	0.03
Woodchip bedding	196	1200	–
Pine boards (*Pinus* spp.)	500	1200	–

There were five different artificial cavity designs tested. Dimensions, design, and construction materials used were similar to those used for a previous fisher den box study (Davis and Horley, 2015). The materials of each artificial cavity included the construction materials of the cavity and 13 cm of wood chip bedding material placed at the bottom of the internal cavity space. Construction materials included pine, aspen, or Douglas fir plywood and extruded polystyrene insulation (Owens Corning, Foamular 250, 1.9 cm, R-4). Four of the artificial cavity types had sides that were constructed of two layers of untreated plywood with polystyrene insulation between them. The fifth artificial cavity type had a single layer of treated plywood, 3.8 cm x 3.8 cm pine boards for an internal frame, and no insulation. Each artificial cavity had a 7.6 cm x 10.2 cm rectangular entrance hole. For each artificial cavity we measured internal cavity volume, total volume of materials, and thickness of each construction material. We used these measurements to calculate the internal air volume, the volume of the construction materials, and the total surface area of the cavity. Density, specific heat capacity, and thermal resistance values for plywood, pine boards, woodchips, and insulation (Table 1) were estimated from literature values or obtained in the lab (Dunlap, 1912; MacLean, 1941; TenWolde et al., 1988; Kamke, 1989; Ragland et al., 1991; Osanyintola et al., 2005; Al-Ajlan, 2006; Asdrubali et al., 2015). Like natural cavities, each artificial cavity type varied in its physical and thermal characteristics (Supplementary S3). The 1.3 cm (1/2 inch) aspen plywood, and 1.6 cm (5/8 inch) Douglas fir plywood cavities were stained to prevent rotting and moisture build-up.

Ambient and internal temperatures were measured at 30 minute intervals for each cavity using temperature loggers (HOBO® UA-001–64 pendant data loggers for 4 natural cavities; or MX2201 for all den boxes and the remaining natural cavities, Onset Computer Corporation, Massachusetts, USA). For both cavity types, ambient temperature loggers were hung at chest height or next to the cavity hole and were housed in two white funnels to prevent the effects of wind and solar radiation. For natural cavities, internal loggers were either hung $\sim$ 5 cm above the bottom of the cavity with fishing line or placed on the bottom of the cavity if the logger could not be hung. Internal loggers were positioned $\sim$ 5 cm above the bedding material in artificial cavities. All loggers were set to measure temperature in degrees Celsius. For modeling, ambient temperatures were converted to Kelvin scale. Modelled temperatures were then converted back to degrees Celsius for data presentation.

We assumed air was moving at a constant velocity through the entrance hole was 0.1 m/s, which is similar to the standard air velocity in houses (Standard, 2005; American Society of Heating, Refrigerating and Air Conditioning Engineers, 2010). This assumption is higher than the air speed found in Wachob's (1996) study on Mountain Chickadee nest boxes (< 0.05 m/s). However, the 25 mm diameter of the entrance hole of the nest boxes in their study was significantly smaller than entrance holes to tree cavities or artificial den boxes we used, which likely restricted air flow between their nests and the outer environment.

The density of air at 1 atmospheric pressure decreases from 1.45 kg/m^3 at -30°C to 1.16 kg/m^3 at 30°C. Isobaric specific heat capacity of air varies from 1003 J/kg*K at -30°C to 1005 J/kg*K at 30°C. For our study, we used a constant air density value of 1.29 kg/m^3 (at 0°C) and constant isobaric specific heat capacity value of 1004 J/kg*K (at 0°C) to fit the model. Using constant values of density and specific heat capacity of air simplifies model computation and has a small effect on model results because the overall heat capacity of air is several orders of magnitude less than the overall heat capacity of the materials.

Based on the cavity-specific physical and thermal parameters and site-specific ambient temperature measurements described above, we modeled the internal temperature of each cavity throughout its measurement period using Eq. (10) (see R script in supplementary materials). We used the first internal temperature measurement as the initial temperature value used for variable $T_{in(t-1)}$. Predicted temperature at time t ($T_{in(t)}$) was then calculated at 30 minute intervals ($\Delta t = 1800$ s) throughout the rest of the monitoring period using modeled internal temperature and measured ambient temperature at time t - 1.

2.4. Data analysis

2.4.1. Assessing model accuracy

We evaluated model accuracy using root mean squared error (RMSE). For each cavity, we calculated model error at each sampling interval as the difference between measured and modeled cavity temperature. Model error was used to calculate daily RMSE for each cavity and an overall RMSE for the entire deployment.

We used three generalized estimating equation models (GEE, $\alpha = 0.05$) to evaluate sources of error in the model. GEEs allowed us to test the generalizability of the model while accounting for the temporal correlation between measurements (Zeger and Liang, 1986). GEE model 1 assessed differences in daily RMSE as a function of cavity type (*cavityType*: Natural or Artificial cavity*)*. GEE model 2 assessed differences in daily RMSE within artificial cavities as a function of artificial cavity types (*ArtificialType*: Artificial cavity types). GEE model 3 assessed differences in daily RMSE within natural cavities as a function of study area (*studyArea*), the total heat capacity of the materials (*Cm*), the total heat transfer coefficient of the cavity sides *(Uw)*, total material volume (*matVol*), outer cavity surface area (*cavSA*), entrance hole area (*holeA*), total cavity diameter (*cavDia*), and average thickness of the wood that makes up the side of the cavity (*sideThickness*). Due to unequal sample sizes, we did not include tree species or tree condition as covariates within GEE model 3. We assessed collinearity between covariates with scatter plot matrices that included locally weighted smoothing and Spearman correlation coefficients. Preliminary analyses identified high collinearity between *subVol* and *cavSA* ($r = 0.87$), *matVol* and *Cs* ($r = 0.93$), and *cavDia* and *sideThickness* ($r = 0.74$). Therefore, we removed *matVol* and cav*Dia* covariates from the model.

For all models, we assumed a Gaussian error distribution and an autoregressive correlation structure that allows higher correlation for daily RMSE values taken closer together than those taken further apart. We also used Tukey's Honest Significant Difference (Tukey's HSD, $\alpha = 0.05$) as a post hoc analysis to make pairwise comparisons. We performed all analyses in R (Version 4.1.1) with package 'geepack' (Halekoh et al., 2006). We assessed assumptions of normality and equal variance using diagnostic plots (quantile-quantile plots, plots of residuals vs. predictor variables, and scale location plots). We also used Cook's distance plots to assess leverage from outliers.

2.4.2. Thermal arrest periods

Results showed that natural cavities exhibited temperature patterns similar to thermal arrest periods identified in solid tree stems. For analysis, a thermal arrest interval was identified when the absolute value of ($T_{in(t)}$ – model error) was less than 1°C. Thermal arrest periods occurred when there were ≥ 2 consecutive thermal arrest intervals. A day for which a thermal arrest period was identified was considered a thermal arrest day. We selected a random subset of all thermal arrest periods identified by this method and manually inspected the predicted and modeled cavity temperatures to confirm a thermal arrest period had occurred.

We identified the ambient and modeled temperatures that were associated with the thermal arrest periods. Because the occurrence of thermal arrest periods is likely related to ambient temperature and the temperature in the tree, we assessed whether ambient and modeled temperature could be used as indicators for thermal arrest periods. We used ambient temperatures between -1 and 1°C for the temperature range when freeze-thaw conditions could occur. To test if these periods significantly affected daily RMSE, we added a fixed covariate, *ThermalArrest,* to GEE model 3 to evaluate differences in daily RMSE between thermal arrest days and days that were not thermal arrest days.

2.4.3. Evaluating bias

We evaluated systematic bias in model results by calculating average daily bias for each sampled artificial cavity, and average daily bias for natural cavities across days with and without a thermal arrest period. We also calculated bias for each thermal arrest period identified.

3. Results

3.1. Model accuracy

We monitored natural cavities for 5884 days (Minnesota; 2953, Michigan; 2931) with 282432 temperature measurements. Average sampling period for natural cavities was 137 (SD = 33) days. Average ambient temperatures ranged from -19.6 °C (SD = 1.4 °C) to 28.0 °C (SD = 2.9 °C) for natural cavities in Michigan, and from -30.1 °C (SD = 15.6 °C) to 27.2 °C (SD = 8.8 °C) for natural cavities in Minnesota. We monitored artificial cavities for 4598 days (220704 temperature measurements), with an average of 166 (SD = 75) days sampled per artificial cavity. Average daily ambient temperature ranged from −32.6 °C (SD = 6.1 °C) to 29.1 °C (SD = 10.7 °C) for artificial cavities. Average absolute difference between ambient and cavity temperature varied between structures from 0.41 to 3.95 °C for natural cavities, and 0.99–3.56 °C for artificial cavities (Supplementary Tables S7, S8 and S9).

Natural cavities had an average RMSE of 1.77 °C (SD = 0.66 °C, range = 0.42–3.65 °C) across the full monitoring periods from both states. Artificial cavities had an average RMSE of 1.02 °C (SD = 0.45 °C, range = 0.42–1.94 °C). The model-predicted internal cavity temperatures were consistent with measured internal cavity temperature and followed daily oscillations in ambient temperature throughout each monitoring period (Fig. 2A–D). Supplementary material S4, S5, and S6 summarize RMSE for each natural and artificial cavity sampled.

Average daily RMSE across all cavities (natural and artificial) monitored was 1.20 °C (SD = 1.03 °C). Daily RMSE was lower for artificial cavities (0.83 °C, SD = 0.63°C, range = 0.04–4.7 °C) than for natural cavities (1.47°C, SD = 1.20°C, range = 0.05–12.56 °C; GEE, Wald = 40.5, $P < 0.001$).

For artificial cavities, there were significant main effects of box design (GEE, $F_{4,\ 4593} = 7.5$, $P < 0.001$). Daily RMSE was slightly higher in the uninsulated 1.9 cm (3/4 inch) pine plywood cavity compared to the insulated 1.9 cm (3/4 inch) pine plywood cavity (Tukey's HSD, $P <$

Table 2
Summary of daily root mean squared error (RMSE) for five artificial cavity types tested.

Cavity Type	Mean	SD	Min	Max
Insulated 1.9 cm Pine plywood	0.62	0.38	0.10	2.09
Insulated 1.3 cm Pine plywood	0.75	0.69	0.05	4.48
Insulated 1.3 cm Aspen plywood	0.92	0.59	0.06	3.02
Insulated 1.6 cm Douglas fir plywood	0.73	0.52	0.04	3.98
Uninsulated 1.9 cm Pine plywood	1.41	0.83	0.12	4.71

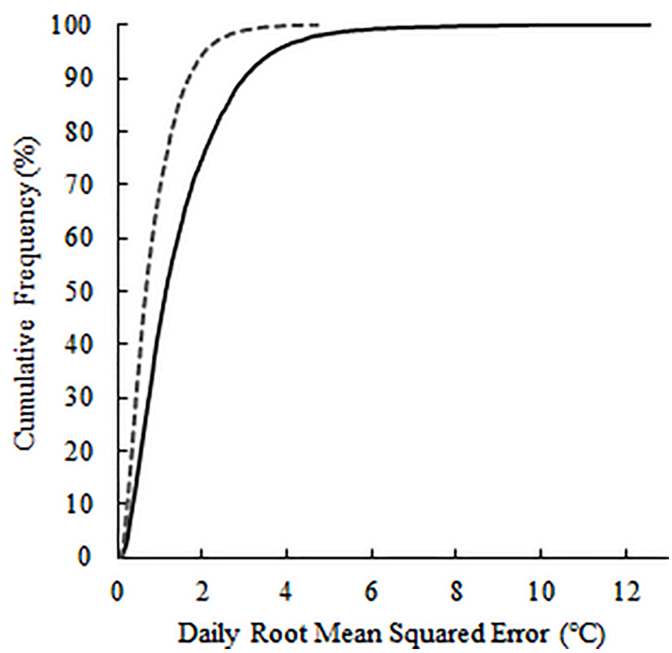

Fig. 3. Cumulative frequency distribution of daily root mean squared error (RMSE) for natural (black line) and artificial cavities (dashed gray line) calculated across all cavities and all monitoring days.

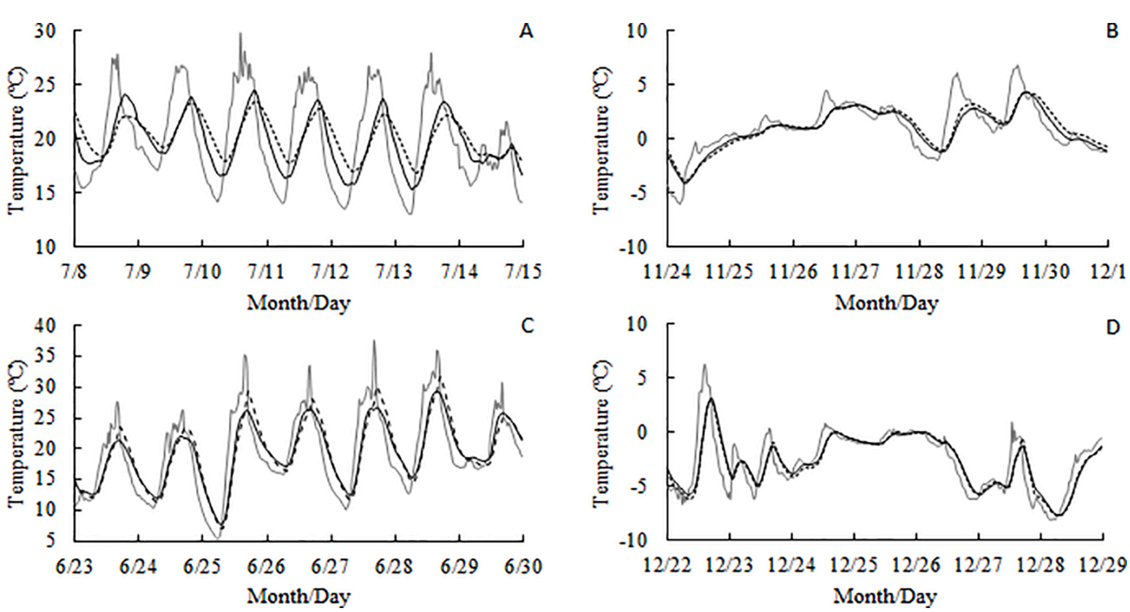

Fig. 2. Results across a sampled week in two natural cavities (A-B) and two artificial cavities (C-D). The solid gray line describes the ambient temperature. Measured temperature in the cavity is expressed with the solid black line. Modeled temperature is expressed as the dashed black line. Fig. A–C occurred in year 2020, Fig. D occurred in 2019.

0.001) and compared to the insulated 1.6 cm (5/8 inch) Douglas fir plywood cavity (Tukey's HSD, $P = 0.01$, Table 2). Daily RMSE was slightly higher in the insulated 1.3 cm (1/2 inch) aspen plywood cavity compared to the insulated 1.9 cm (3/4 inch) pine plywood cavity (Tukey's HSD, $P = 0.02$, Table 2).

For natural cavities, there were no significant main effects for study area (*studyArea*, Wald = 1.26, $P = 0.26$), the total heat capacity of the materials (*Cm*, $\beta < 0.001$, Wald = 0.346, $P = 0.56$), the total heat transfer coefficient of the cavity sides (*Uw*, $\beta = -0.34$, Wald = 1.59, $P = 0.21$), the outer surface area of the cavity (*cavSA*, β = -0.08, Wald = 0.46, $P = 0.50$), the entrance hole area (*holeA*, $\beta = 27.7$, Wald = 3.41, $P = 0.06$), or the average thickness of the wood on the side of the cavity (*sideThickness*, $\beta = -3.24$, Wald = 0.60, $P = 0.44$).

For natural cavities, 75% of sampled days (4413 days) had less than 2 °C RMSE (Fig. 3) when days with and without thermal arrest periods were included in calculations. Of the 1471 days with RMSE greater than 2 °C, almost half (716 days) were days with a thermal arrest period and about 20% (272 days) occurred within 48 hours after a day that contained the end of a thermal arrest period. The 483 days with RMSE greater than 2 °C that were greater than 48 hours after a thermal arrest period ended occurred across a broad range of average ambient temperatures (mean = -5.23 °C, SD = 16.1 °C, range = -30.2–24.9 °C). Overall, for natural cavities 92% of all sampled days either had RMSE less than 2, contained a thermal arrest period, or occurred within 48 hours of thermal arrest period, while 8% of all sampled days had RMSE greater than 2 outside of a thermal arrest period.

For artificial cavities, 95% of sampled days (4347 days) had less than 2 °C RMSE (Fig. 3). Days with RMSE greater than 2 °C occurred across a broad range of average ambient temperatures (mean = 3.95 °C, SD = 11.9 °C, range = -26.3–24.3 °C). About half (46%) of all days with RMSE greater than 2 °C occurred in the artificial cavity without foam insulation, and 20% of all days with RMSE greater than 2 °C occurred in the 1.3 cm (1/2 inch) aspen plywood artificial cavity.

3.2. Thermal arrest periods

There were 1843 thermal arrest periods over 2343 days identified in natural cavities (Minnesota: 807; Michigan: 1036, Fig. 4). In Minnesota, thermal arrest periods accounted for 11% of the intervals sampled, while in Michigan they accounted for 33% of the intervals sampled. On average thermal arrest periods lasted for 17 hours (median = 6 hours, SD = 43.8 hours, range = 1–1235 hours) with 70% of all thermal arrest periods lasting less than 12 hours, 10% of thermal arrest periods lasting between 12 and 20 hours, and 10% of thermal arrest periods lasting between 20 and 48 hours.

Average thermal arrest period temperature was -0.11°C (SD = 0.44, range = -0.99–0.98). Thermal arrest periods followed expected phase change dynamics, in that temperature stabilized every time the cavity reached temperatures between -1 and 1 °C. In many cases, especially during long thermal arrest periods, ambient and modeled temperatures oscillated between positive and negative temperatures during the thermal arrest period (e.g. Fig. 4B). The longest thermal arrest period lasted 1234.5 hours (~51 days), ambient temperature oscillated above and below freeze-thaw temperatures 69 times, and modeled temperature oscillated between freeze-thaw temperatures 13 times. The number of oscillations was positively correlated with the length of the thermal arrest period.

There were significant main effects for days that exhibited thermal arrest (*ThermalArrest*) (GEE, Wald = 9.87, $P = 0.002$). Days without thermal arrest periods had slightly lower RMSE (1.34 °C, SD = 1.02 °C, range = 0.06–8.11 °C) than days with a thermal arrest period (1.68 °C, SD = 1.39 °C, range = 0.05–12.56 °C). Nonetheless, most thermal arrest periods had low error. For example, 69% of days with a thermal arrest period had less than 2 °C RMSE, and 87% of days with a thermal arrest period had less than 3 °C RMSE. In contrast, 79% of days without a thermal arrest period had less than 2 °C RMSE, and 92% had less than 3 °C RMSE.

We found that modeled temperature was a relatively strong indicator of thermal arrest periods. A thermal arrest period occurred on 88% of days when modeled cavity temperatures were between -1 and 1°C. Ambient temperature was a weaker indicator of when a thermal arrest period would occur. A thermal arrest period occurred on 63% of days when ambient temperatures were between -1 and 1°C.

3.3. Bias

Average daily bias for artificial cavities was -0.06 °C (SD = 0.30, range = -0.85–0.34). For natural cavities, average daily bias for days that did not have a thermal arrest period was 0.06 °C (SD = 0.51, range = -1.13–1.40). Average daily bias for days with a thermal arrest period was -0.49 °C (SD = 0.48, range = -1.40–0.34). Average bias for thermal arrest periods was -0.56 °C (SD = 1.84, range = -10.1–9.98).

4. Discussion

The temperature in a tree cavity system is governed by complex interactions between energy transfer processes, ambient conditions, habitat characteristics, and physical and biological properties of the cavity. The described model simplifies these complex interactions into two main modes of energy transfer that can be calculated from a relatively small set of input parameters. Despite the simplifying assumptions that the model is based on, it accurately predicted cavity temperature for both natural and artificial cavities for several months across broad ambient temperature ranges. Our sampling period RMSE values were similar to RMSE values for more complex thermal models predicting the temperature within solid tree stems (Potter and Andresen, 2002; Reid

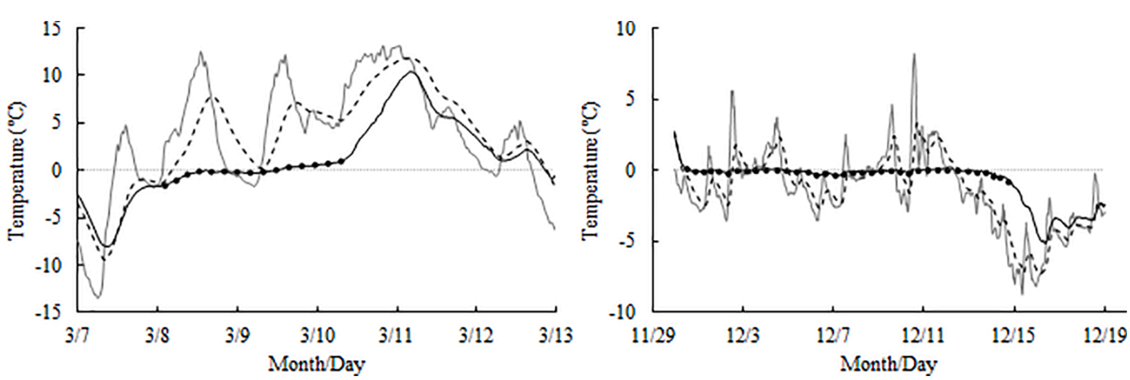

Fig. 4. Multiple day results of natural cavities with thermal arrest periods at 0 °C. The solid gray line describes the ambient temperature. Modeled temperature is expressed as the dashed black line. Measured temperature in the cavity is expressed with the solid black line. The thermal arrest period(s) is expressed as the large dotted black line. The dotted horizontal gray line represents 0° Figures A occurred in year 2021, while Fig. B occurred in 2020.

et al., 2020). RMSE values were also similar to RMSE values for a complex thermal model used to predict microclimate temperature throughout snow and soil profiles (NicheMapR; Kearney et al. 2014; Kearney and Porter 2017, Fitzpatrick et al. 2019; Kearney 2020). Additionally, GEE analyses showed that our model performed consistently in cavities with different thermal and physical characteristics and across two study areas with different thermal conditions. This suggests that the model can be applied to cavities in different tree species, different cavity sizes, and forest conditions. We also found almost no bias in error for both artificial and natural cavities, indicating that there were no systematic tendencies such as effects of radiation and convection that caused differences between modeled and measured temperatures. This further shows that the energy processes included in the model are likely the most important processes governing cavity temperatures.

We found the model predicted temperatures in artificial cavities better than in natural cavities. Thermal arrest periods accounted for some of the error in natural cavities, but differences are also likely related to increased error when measuring the physical characteristics of natural cavities. Surface area and volume of natural cavities, for example, could not be measured as precisely as surface area and volume of artificial cavities. Because the model predicts temperature as a function of the physical and thermal characteristics of the cavity, any error in estimates of cavity characteristics could contribute to error in the model. Other simplifying assumptions, such as our assumption that each natural cavity was a perfect cylinder, or the ceiling and floor were the same thickness as the outer side, would contribute to model error for natural cavities. Future work could focus on methods that would allow more precise estimates of natural cavity characteristics. For example, accuracy could potentially improve by cutting down the cavities to obtain accurate measurements of the physical properties of cavities. However, given the concerns over availability of large trees with cavities (e.g., Lindenmayer et al. 2012), and that error was relatively low, non-invasive sampling methods are likely sufficient for parameterizing the model.

The uninsulated 1.9 cm (3/4 inch) pine plywood cavity and the insulated 1.3 cm (1/2 inch) aspen plywood cavity had slightly higher daily RMSE than the other cavity types and contributed to the highest number of days with RMSE greater than 2°C. Higher error in the uninsulated 1.9 cm (3/4 inch) pine plywood cavity may be attributed to its lack of insulation, making it less thermally stable, and more prone to effects of radiation or convection on cavity temperature than the other artificial cavity types. Nonetheless, differences in RMSE were small among all artificial cavity types, indicating that error caused by differences in plywood thicknesses and plywood tree species were small relative to random effects such as differences in sample size, location of boxes, sampling period length, or other factors that could affect RMSE.

4.1. Thermal arrest periods

We found 40% of days sampled had a period where natural cavity temperatures exhibited a thermal arrest phenomenon, mimicking the fundamental dynamics of phase change described in previous studies (Graf et al., 2015; Zhao et al., 2021). When cavity temperatures reached freeze-thaw temperatures (between -1 and 1 °C), a thermal arrest period began and temperatures in the cavity remained within freeze-thaw for extended periods of time. When a thermal arrest period ended, measured temperatures would then gradually return to expected temperatures in the absence of freeze-thaw temperatures. Because there has not been any documentation of this phenomenon occurring in tree cavities, the exact mechanism of how thermal arrest periods occur in the internal cavity space is unknown. We expect that the mechanism is similar to that of solid trees, where water or sap in the wood undergoes a phase change when temperatures reach freeze-thaw temperatures, creating a thermal arrest period in the wood temperature (Derby and Gates, 1966; Graf et al., 2015; Charrier et al., 2017; Reid et al., 2020; Zhao et al., 2021). For tree cavities, we believe that during this period, there is an exchange in energy between the water/sap, the wood surrounding the cavity space, and the air within the cavity, resulting in the entire tree cavity system exhibiting a period of thermal arrest. Future work, however, should verify the mechanisms driving the thermal arrest periods we identified in this study.

Thermal arrest periods did not occur in artificial cavities. This could be because artificial cavities maintain drier microclimate conditions than natural cavities (McComb and Noble, 1981a; Maziarz et al., 2017) and therefore may not have enough water content for thermal arrests to occur. Further, construction materials have lower moisture content than green wood in standing trees (Skaar, 2012). The water repellent chemicals in wood preservatives would also result in drier conditions in artificial cavity walls.

The model does not directly account for phase change processes at freeze-thaw temperatures, and therefore cannot predict thermal arrest periods. Consequently, days that had a thermal arrest period had higher daily RMSE and accounted for proportionately more days that had RMSE greater than 2°C. Differences in average daily RMSE between days that had a thermal arrest period and days that did not have a thermal arrest period were less than 0.4°C. There was also a large proportion (69%) of thermal arrest days with RMSE less than 2°C, indicating the model can produce acceptable results at the daily scale during freeze-thaw conditions.

Predicting thermal arrest periods would decrease model error under freeze-thaw conditions. Phase change dynamics in trees, however, are complicated by differences in structure, cells, and tissues within and between individual trees and tree species (Lintunen et al., 2013; Charrier et al., 2017; Reid et al., 2020; Zarrinderakht et al., 2021). Patterns are also influenced by other factors such as microclimate (i.e., temperature and humidity), topography, or how much water or sap is in the system (Graf et al., 2015; Charrier et al., 2017). Reid et al. (2020) described a model that can predict temperatures throughout tree stems using transient heat flow processes. In their model they account for phase changes of water by assigning the sapwood a large pseudo-specific heat capacity when the cavity reaches a specific temperature interval in which phase change is expected to happen. In a simulation they found the model predicted a thermal arrest with little error (RMSE = 0.9 °C). Adapting their technique to the model described in this paper could be useful but may be difficult given that the foundation of our model is based on lumped capacitance energy transfer and not transient energy transfer.

Thermal arrest periods in cavities can affect cavity selection and animal thermoregulation. For example, if cavities remain stable around freeze-thaw while ambient temperatures rise above freeze-thaw, the thermal benefit of thermal arrest periods to animals is lower. Conversely, if ambient temperatures fall below freeze-thaw while a cavity is experiencing a thermal arrest in temperature, an animal would benefit by selecting that cavity. The effect of body heat from an animal would tend to make a cavity warmer (Maziarz, 2019). At temperatures slightly above freeze-thaw, the added body heat would delay or prevent a thermal arrest period. In contrast, at temperatures slightly below freeze-thaw, added body heat could increase the probability or alter the length of a thermal arrest period. Despite a large range and high standard deviation of bias values across the thermal arrest periods, the average bias across all thermal arrest periods was close to 0°C. This indicates that the net thermoregulatory cost of selecting a cavity that experiences multiple thermal arrest periods is close to zero.

4.2. Model applications

The model we describe in this study is a useful tool that allows us to predict a cavity's temperature, providing the opportunity to understand the effects of cavity thermal environment on habitat selection or physiology of cavity-dependent animals. For example, the model can be used to understand the effects of temperature on the development and growth of offspring, or energy needed to regulate body temperature (Kendeigh, 1961; Du Plessis et al., 1994; Zalewski, 1997; Sedgeley, 2001; Wiebe and Swift, 2001; Ardia et al., 2006; Clement and Castleberry, 2013; Joyce, 2013; Matthews et al., 2019).

Researchers can adjust the model's input parameters to create different cavity scenarios. For example, the parameters that are associated with the cavity's thermal and physical characteristics can be adjusted to predict temperatures in cavities that vary in size and wood type. Having the ability to adjust model parameters can also be useful for understanding how a cavity's temperature changes over time as its thermal and physical characteristics change through decay, or from cavity excavators (Edworthy and Martin, 2014). Researchers can also adjust ambient temperature conditions and predict historical and future cavity temperatures. This would be especially useful when understanding the direct effects of climate changes on cavity microclimate and associated effects on behavior and physiology of the species that use cavities.

Lately there has been increased interest in using nest boxes as a management tool in areas where natural cavities are limited (Goldingay et al., 2015). For nest boxes to be an effective alternative, they must mimic the overall function and microclimate of the natural cavities in the areas of interest (Griffiths et al., 2018). Researchers can create multiple designs of nest boxes and use the model to estimate the internal temperature and determine which nest box design is best, without having to build and install them and then measure their internal temperature (Goldingay et al., 2015; Larson et al., 2018).

The framework of this model may also be useful for predicting the temperature of other enclosed microsites. For example, the temperature of hollow logs, squirrel dreys, or enclosed nests could potentially be estimated by treating them as a lumped capacitance reservoir of heat and using similar simplifying assumptions we used to model tree cavities. However, other energy processes may play an important role in these systems. Testing and verifying the model on these systems would be needed.

5. Conclusion

The model described in this paper is useful for predicting cavity temperatures. It is computationally simple and easy to parameterize relative to other microclimate models (e.g. NicheMapR). It was generalizable across two study areas, in different tree species, in different cavity sizes, and in natural and artificial cavities. Although we tested this model in cavities used by martens and fishers, the model's ability to predict cavity temperatures across a relatively broad range of conditions should allow it to model temperatures in cavities that are used by other animal species. Further, the thermal model could be a useful tool for ecological applications such as understanding animal response to cavity temperature. For example, researchers can use our model to understand how differences in cavity characteristics influence cavity microclimate and selection by animals. Similarly, our model can be used to predict temporal changes in cavity temperatures, which can be important for understanding cavity use in response to changes in climate.

CRediT authorship contribution statement

Taylor B. Velander: Conceptualization, Methodology, Data curation, Validation, Formal analysis, Writing – original draft, Writing – review & editing. **Michael J. Joyce:** Conceptualization, Funding acquisition, Methodology, Data curation, Writing – review & editing, Supervision. **Angela M. Kujawa:** Conceptualization, Data curation, Writing – review & editing. **Robert L. Sanders:** Conceptualization, Funding acquisition, Data curation, Writing – review & editing. **Paul W. Keenlance:** Conceptualization, Funding acquisition, Writing – review & editing. **Ron A. Moen:** Conceptualization, Methodology, Formal analysis, Writing – review & editing, Supervision.

Declaration of Competing Interest

The authors declare that they have no known competing financial interests or personal relationships that could have appeared to influence the work reported in this paper.

Data availability

Data will be made available on request.

Acknowledgments

We thank Michael McMahon for helping collect field data and Dr. Guy Sander for his in-depth feedback on this project. This work was supported by the Minnesota Environmental and Natural Resources Trust Fund as recommended by the Legislative-Citizen Commission on Minnesota's Resources, the Great Lakes Restoration Initiative administered by the Bureau of Indian Affairs, and by a summer research assistantship from the Integrated Biosciences graduate program, University of Minnesota-Duluth.

Supplementary materials

Supplementary material associated with this article can be found, in the online version, at doi:10.1016/j.ecolmodel.2023.110302.

References

Al-Ajlan, S.A., 2006. Measurements of thermal properties of insulation materials by using transient plane source technique. Appl. Therm. Eng. 26, 2184–2191. https://doi.org/10.1016/j.applthermaleng.2006.04.006.

Amat-Valero, M., Calero-Torralbo, M.A., Václav, R., Valera, F., 2014. Cavity types and microclimate: implications for ecological, evolutionary, and conservation studies. Int. J. Biometeorol. 58, 1983–1994. https://doi.org/10.1007/s00484-014-0801-0.

American Society of Heating, Refrigerating and Air Conditioning Engineers, 2010. ASHRAE Standard Thermal Environmental Conditions for Human Occupancy. The Society.

Ardia, D.R., Pérez, J.H., Clotfelter, E.D., 2006. Nest box orientation affects internal temperature and nest site selection by tree swallows. J. Ornithol. 77, 339–344. https://doi.org/10.1111/j.1557-9263.2006.00064.x.

Asdrubali, F., D'Alessandro, F., Schiavoni, S., 2015. A review of unconventional sustainable building insulation materials. Sustain. Mater. Technol. 4, 1–17. https://doi.org/10.1016/j.susmat.2015.05.002.

Aubry, K.B., Raley, C.M., Buskirk, S.W., Zielinski, W.J., Schwartz, M.K., Golightly, R.T., Purcell, K.L., Weir, R.D., Yaeger, J.S., 2013. Meta-analyses of habitat selection by fishers at resting sites in the pacific coastal region. J. Wildl. Manag. 77, 965–974. https://doi.org/10.1002/jwmg.563.

Berg, S., Erb, J., Spaid, V., Dewey, D., Coy, P., Sampson, B., Fieberg, J., Arnold, T., Forester, J., 2020. The role of local cavity tree density in the selection of den sites by female fishers (Pekania pennanti) in northern Minnesota. Can. J. For. Res. 50, 742–750.

Bergman, T.L., Incropera, F.P., Lavine, A.S., Dewitt, D.P., 2011. Introduction to Heat Transfer. John Wiley Sons.

Berry, R., Livesley, S., Aye, L., 2013. Tree canopy shade impacts on solar irradiance received by building walls and their surface temperature. Build. Environ. 69, 91–100.

Bolstad, P.V., Bentz, B.J., Logan, J.A., 1997. Modelling micro-habitat temperature for Dendroctonus ponderosae (Coleoptera: scolytidae). Ecol. Model. 94, 287–297. https://doi.org/10.1016/S0304-3800(96)00021-X.

Bryant, S.R., Shreeve, T.G., 2002. The use of artificial neural networks in ecological analysis: estimating microhabitat temperature. Ecol. Entomol. 27, 424–432. https://doi.org/10.1046/j.1365-2311.2002.00422.x.

Charrier, G., Nolf, M., Leitinger, G., Charra-Vaskou, K., Losso, A., Tappeiner, U., Améglio, T., Mayr, S., 2017. Monitoring of freezing dynamics in trees: a simple phase shift causes complexity. Plant Physiol. 173, 2196–2207. https://doi.org/10.1104/pp.16.01815.

Clement, M.J., Castleberry, S.B., 2013. Tree structure and cavity microclimate: implications for bats and birds. Int. J. Biometeorol. 57, 437–450. https://doi.org/10.1007/s00484-012-0569-z.

Cockle, K.L., Martin, K., Wesołowski, T., 2011. Woodpeckers, decay, and the future of cavity-nesting vertebrate communities worldwide. Front. Ecol. Environ. 9, 377–382. https://doi.org/10.1890/110013.

Cohen, J., 1994. Snow cover and climate. Weather 49, 150–156. https://doi.org/10.1002/j.1477-8696.1994.tb05997.x.

Coombs, A.B., Bowman, J., Garroway, C.J., 2010. Thermal properties of tree cavities during winter in a northern hardwood forest. J. Wildl. Manag. 74, 1875–1881. https://doi.org/10.2193/2009-560.
Cui, B., Fan, C., Munk, J., Mao, N., Xiao, F., Dong, J., Kuruganti, T., 2019. A hybrid building thermal modeling approach for predicting temperatures in typical, detached, two-story houses. Appl. Energy 236, 101–116. https://doi.org/10.1016/j.apenergy.2018.11.077.
Davis, L.R., Horley, S., 2015. Fisher (Pekania pennanti) Artificial Reproductive Den Box Study. Williams Lake, British Columbia, Canada.
De Frenne, P., Zellweger, F., Rodríguez-Sánchez, F., Scheffers, B.R., Hylander, K., Luoto, M., Vellend, M., Verheyen, K., Lenoir, J., 2019. Global buffering of temperatures under forest canopies. Nat. Ecol. Evol. 3, 744–749. https://doi.org/10.1038/s41559-019-0842-1.
Derby, R.W., Gates, D.M., 1966. The temperature of tree trunks-calculated and observed. Am. J. Bot. 53, 580–587. https://doi.org/10.1002/j.1537-2197.1966.tb07374.x.
Du Plessis, M.A., Weathers, W.W., Koenig, W.D., 1994. Energetic benefits of communal roosting by acorn woodpeckers during the nonbreeding season. Condor 96, 631–637. https://doi.org/10.2307/1369466.
Dunlap, F., 1912. The specific heat of wood. US Dep. Agric. For. Serv. 110.
Edworthy, A.B., Martin, K., 2014. Long-term dynamics of the characteristics of tree cavities used for nesting by vertebrates. For. Ecol. Manag. 334, 122–128. https://doi.org/10.1016/j.foreco.2014.09.001.
Erb, J., Coy, P., Sampson, B., 2015. Reproductive ecology of fisher and marten in Minnesota.
Fawcett, S., Sistla, S., Dacosta-Calheiros, M., Kahraman, A., Reznicek, A.A., Rosenberg, R., von Wettberg, E.J.B., 2019. Tracking microhabitat temperature variation with iButton data loggers. Appl. Plant Sci. 7, 1–12. https://doi.org/10.1002/aps3.1237.
Fitzpatrick, M.J., Zuckerberg, B., Pauli, J.N., Kearney, M.R., Thompson, K.L., Werner, L. C., Porter, W.P., 2019. Modeling the distribution of niche space and risk for a freeze-tolerant Ectotherm, Lithobates Sylvaticus. Ecosphere 10. 10.1002/ecs2.2788.
Gilad-Bachrach, R., Navot, A., Tishby, N., 2003. An information theoretic tradeoff between complexity and accuracy, in: Lecture Notes in Computer Science. pp. 595–609.
Goldingay, R.L., Rueegger, N.N., Grimson, M.J., Taylor, B.D., 2015. Specific nest box designs can improve habitat restoration for cavity-dependent arboreal mammals. Restor. Ecol. 23, 482–490. https://doi.org/10.1111/rec.12208.
Graf, I., Ceseri, M., Stockie, J.M., 2015. Multiscale model of a freeze-thaw process for tree sap exudation. J. R. Soc. Interface 12. https://doi.org/10.1098/rsif.2015.0665.
Griffiths, S.R., Lentini, P.E., Semmens, K., Watson, S.J., Lumsden, L.F., Robert, K.A., 2018. Chainsaw-carved cavities better mimic the thermal properties of natural tree hollows than nest boxes and log hollows. Forests 9. https://doi.org/10.3390/f9050235.
Grüebler, M.U., Widmer, S., Korner-Nievergelt, F., Naef-Daenzer, B., 2014. Temperature characteristics of winter roost-sites for birds and mammals: tree cavities and anthropogenic alternatives. Int. J. Biometeorol. 58, 629–637. https://doi.org/10.1007/s00484-013-0643-1.
Halekoh, U., Højsgaard, S., Yan, J., 2006. The R Package geepack for Generalized Estimating Equations. J. Stat. Softw. 1–11, 15/2.
Hedlund, H., Johansson, P., 2000. Heat capacity of birch determined by calorimetry: implications for the state of water in plants. Thermochim. Acta 349, 79–88.
Hietaharju, P., Ruusunen, M., Leivisk, K., 2018. A dynamic model for indoor temperature prediction in buildings. Energies 11. https://doi.org/10.3390/en11061477.
Howe, S., Kilgore, D.L., Colby, C., 1987. Respiratory gas concentrations and temperatures within nest cavities of the northern flicker (Colaptes auratus). Can. J. Zool. 65, 1541–1547. https://doi.org/10.1139/z87-238.
Hudson, G., Underwood, C., 1982. A Simple Building Modelling Procedure for Matlab /Simulink G. Underwood Department of the Built Environment Newcastle upon Tyne UK ABSTRACT, pp. 1–7. Hudson & C . P.
International Standard, 2005. ISO Standard Ergonomics of the Thermal Environment - Analytical Determination and Interpretation of Thermal Comfort Using Calculation of the PMV and PPD Indices and Local Thermal Comfort Criteria. International Standards Organization, Geneva, Switzerland.
Isaac, J.L., De Gabriel, J.L., Goodman, B.A., 2008. Microclimate of daytime den sites in a tropical possum: implications for the conservation of tropical arboreal marsupials. Anim. Conserv. 11, 281–287. https://doi.org/10.1111/j.1469-1795.2008.00177.x.
Joyce, M.J., 2013. Space use behavior and multi-scale habitat selection of American marten (Martes americana) in northeastern Minnesota.
Kamke, F.A., Hasselman, D.P.H., Thomas, J.R., 1989. Thermal conductivity of wood-based panels. Thermal Conductivity 20. Springer US, Boston, MA, pp. 249–259. https://doi.org/10.1007/978-1-4613-0761-7_24.
Kearney, M.R., 2020. How will snow alter exposure of organisms to cold stress under climate warming? Glob. Ecol. Biogeogr. 29, 1246–1256. https://doi.org/10.1111/geb.13100.
Kearney, M.R., Porter, W.P., 2017. NicheMapR – an R package for biophysical modelling: the microclimate model. Ecography 40, 664–674. https://doi.org/10.1111/ecog.02360 (Cop.).
Kearney, M.R., Shamakhy, A., Tingley, R., Karoly, D.J., Hoffmann, A.A., Briggs, P.R., Porter, W.P., 2014. Microclimate modelling at macro scales: a test of a general microclimate model integrated with gridded continental-scale soil and weather data. Methods Ecol. Evol. 5, 273–286. https://doi.org/10.1111/2041-210X.12148.
Kendeigh, C., 1961. Energy of birds conserved by roosting in cavities. Wilson Bull. 73, 140–147.
Kossak, B., Stadler, M., 2015. Adaptive thermal zone modeling including the storage mass of the building zone. Energy Build. 109, 407–417. https://doi.org/10.1016/j.enbuild.2015.10.016.
Kudriavtcev, S., Paramonov, V., Sakharov, I., 2016. Strengthening thawed permafrost base railway embankments cutting berms. In: Proceedings of the MATEC Web Conference, p. 73. https://doi.org/10.1051/matecconf/20167305002.
Larson, E.R., Eastwood, J.R., Buchanan, K.L., Bennett, A.T.D., Berg, M.L., 2018. Nest box design for a changing climate: the value of improved insulation. Ecol. Manag. Restor. 19, 39–48. https://doi.org/10.1111/emr.12292.
Lausen, C.L., Barclay, R.M.R., 2003. Thermoregulation and roost selection by reproductive female big brown bats (Eptesicus fuscus) roosting in rock crevices. J. Zool. 260, 235–244. https://doi.org/10.1017/S0952836903003686.
Leuzinger, S., Vogt, R., Körner, C., 2010. Tree surface temperature in an urban environment. Agric. For. Meteorol. 150, 56–62. https://doi.org/10.1016/j.agrformet.2009.08.006.
Lindenmayer, D.B., Blanchard, W., McBurney, L., Blair, D., Banks, S., Likens, G.E., Franklin, J.F., Laurance, W.F., Stein, J.A.R., Gibbons, P., 2012. Interacting factors driving a major loss of large trees with cavities in a forest ecosystem. PLoS One 7. https://doi.org/10.1371/journal.pone.0041864.
Lintunen, A., Hölttä, T., Kulmala, M., 2013. Anatomical regulation of ice nucleation and cavitation helps trees to survive freezing and drought stress. Sci. Rep. 3, 1–7. https://doi.org/10.1038/srep02031.
Maclean, I.M.D., Suggitt, A.J., Wilson, R.J., Duffy, J.P., Bennie, J.J., 2017. Fine-scale climate change: modelling spatial variation in biologically meaningful rates of warming. Glob. Chang. Biol. 23, 256–268. https://doi.org/10.1111/gcb.13343.
MacLean, J., 1941. Thermal conductivity of wood. Heat. Pip. Air Cond. 13, 380–391.
Mänd, R., Tilgar, V., Lõhmus, A., Leivits, A., 2005. Providing nest boxes for hole-nesting birds - does habitat matter? Biodivers. Conserv. 14, 1823–1840. https://doi.org/10.1007/s10531-004-1039-7.
Matthews, S.M., Green, D.S., Higley, J.M., Rennie, K.M., Kelsey, C.M., Green, R.E., 2019. Reproductive den selection and its consequences for fisher neonates, a cavity-obligate mustelid. J. Mammal. 100, 1305–1316. https://doi.org/10.1093/jmammal/gyz069.
Maziarz, M., 2019. Breeding birds actively modify the initial microclimate of occupied tree cavities. Int. J. Biometeorol. 63, 247–257. https://doi.org/10.1007/s00484-018-01658-x.
Maziarz, M., Broughton, R.K., Wesołowski, T., 2017. Microclimate in tree cavities and nest-boxes: implications for hole-nesting birds. For. Ecol. Manag. 389, 306–313. https://doi.org/10.1016/j.foreco.2017.01.001.
McComb, W.C., Noble, R.E., 1981a. Microclimates of nest boxes and natural cavities in bottomland hardwoods. J. Wildl. Manag. 45, 284–289.
McComb, W.C., Noble, R.E., 1981b. Herpetofaunal use of natural tree cavities and nest boxes. Wildl. Soc. Bull. 261–267.
Méndez-Toribio, M., Meave, J.A., Zermeño-Hernández, I., Ibarra-Manríquez, G., 2016. Effects of slope aspect and topographic position on environmental variables, disturbance regime and tree community attributes in a seasonal tropical dry forest. J. Veg. Sci. 27, 1094–1103. https://doi.org/10.1111/jvs.12455.
Mersten-Katz, C., Barnea, A., Yom-Tov, Y., Ar, A., 2012. The woodpecker's cavity microenvironment: advantageous or restricting? Avian Biol. Res. 5, 227–237. https://doi.org/10.3184/174751912X13530894822224.
Moore, A.D., 1945. Winter night habits of birds. Wilson Bull. 57, 253–260.
Osanyintola, O.F., Talukdar, P., Simonson, C., 2005. Experimental and numerical studies of transient heat and moisture transfer within spruce plywood 0, 1–14.
Paclík, M., Weidinger, K., 2007. Microclimate of tree cavities during winter nights - implications for roost site selection in birds. Int. J. Biometeorol. 51, 287–293. https://doi.org/10.1007/s00484-006-0067-2.
Potter, B.E., Andresen, J.A., 2002. A finite-difference model of temperatures and heat flow within a tree stem. Can. J. For. Res. 32, 548–555. https://doi.org/10.1139/x01-226.
Radmanović, K., Dukić, I., Pervan, S., 2014. Specific heat capacity of wood. Drv. Ind. 65, 151–157. https://doi.org/10.5552/drind.2014.1333.
Ragland, K.W., Aerts, D.J., Baker, A.J., 1991. Properties of wood for combustion analysis. Bioresour. Technol. 37, 161–168. doi.org/10.1016/0960-8524(91)90205-X.
Reid, S., Driller, T., Watson, M., 2020. A two-dimensional heat transfer model for predicting freeze-thaw events in sugar maple trees. Agric. For. Meteorol. 294, 108139 https://doi.org/10.1016/j.agrformet.2020.108139.
Repola, J., 2006. Models for Vertical Wood Density of Scots Pine, Norway Spruce and Birch Stems, and Their Application to Determine Average Wood Density. Silva Fenn, p. 40.
Ruczyński, I., 2006. Influence of temperature on maternity roost selection by noctule bats (Nyctalus noctula) and Leisler's bats (N. leisleri) in Białowieża Primeval Forest, Poland. Can. J. Zool. 84, 900–907. https://doi.org/10.1139/Z06-060.
Sanders, R.L., Cornman, A., Keenlance, P., Jacquot, J.J., Unger, D.E., Spriggs, M., 2017. Resting site characteristics of American marten in the northern lower Peninsula of Michigan. Am. Midl. Nat. 177, 211–225. https://doi.org/10.1674/0003-0031-177.2.211.
Sedgeley, J.A., 2001. Quality of cavity microclimate as a factor influencing selection of maternity roosts by a tree-dwelling bat, Chalinolobus tuberculatus, in New Zealand. J. Appl. Ecol. 38, 425–438. https://doi.org/10.1046/j.1365-2664.2001.00607.x.
Singh, V.K., Tiwari, K.N., 2017. Prediction of greenhouse micro-climate using artificial neural network. Appl. Ecol. Environ. Res. 15, 767–778. https://doi.org/10.15666/aeer/1501_767778.
Skaar, C., 2012. Wood-Water Relations. Springer Science & Business Media.
Suggitt, A.J., Gillingham, P.K., Hill, J.K., Huntley, B., Kunin, W.E., Roy, D.B., Thomas, C. D., 2011. Habitat microclimates drive fine-scale variation in extreme temperatures. Oikos 120, 1–8. https://doi.org/10.1111/j.1600-0706.2010.18270.x.
TenWolde, A., McNatt, J.D., Krahn, L., 1988. Thermal properties of wood and wood panel products for use in buildings. For. Serv. Madison. WI (USA). For. Prod. Lab.

Thompson, K.L., Zuckerberg, B., Porter, W.P., Pauli, J.N., 2018. The phenology of the subnivium. Environ. Res. Lett. 13 https://doi.org/10.1088/1748-9326/aac670.
van der Hoek, Y., Gaona, G.V., Martin, K., 2017. The diversity, distribution and conservation status of the tree-cavity-nesting birds of the world. Divers. Distrib. 23, 1120–1131. https://doi.org/10.1111/ddi.12601.
Vonhof, M.J., Barclay, R.M., 1997. Use of tree stumps as roosts by the western long-eared bat. J. Wildl. Manag. 674–684.
Wachob, D.G., 1996. A microclimate analysis of nest-site selection by mountain chickadees (Un Analisis Microclimatico de la Seleccion de Nidos en Parus gambeli). J. Ornithol. 67, 525–533.
Westermann, S., Schuler, T.V., Gisnas, K., Etzelmüller, B., 2013. Transient thermal modeling of permafrost conditions in Southern Norway. Cryosphere 7, 719–739. https://doi.org/10.5194/tc-7-719-2013.
Wiebe, K.L., 2001. Microclimate of tree cavity nests: is it important for reproductive success in northern flickers? Auk 118, 412–421. https://doi.org/10.2307/4089802.
Wiebe, K.L., Swift, T.L., 2001. Clutch size relative to tree cavity size in Northern Flickers. J. Avian Biol. 32, 167–173. https://doi.org/10.1034/j.1600-048X.2001.320210.x.
Zalewski, A., 1997. Factors affecting selection of resting site type by pine marten in primeval deciduous forests (Bialowieza National Park, Poland). Acta Theriol. 42, 271–288.
Zarrinderakht, M., Konrad, I., Wilmot, T.R., Perkins, T.D., van den Berg, A., Stockie, J.M., 2021. Experimental and computational comparison of freeze-thaw induced pressure generation in red and sugar maple.
Zeger, L., Liang, S., 1986. Longitudinal data analysis for discrete and continuous outcomes. Biometrics 42, 121–130.
Zhang, M., Zhang, X., Lai, Y., Lu, J., Wang, C., 2020. Variations of the temperatures and volumetric unfrozen water contents of fine-grained soils during a freezing–thawing process. Acta Geotech. 15, 595–601. https://doi.org/10.1007/s11440-018-0720-z.
Zhao, Yue, Tian, H., Han, Q., Gu, J., Zhao, Yandong, 2021. Real-time monitoring of water and ice content in plant stem based on latent heat changes. Agric. For. Meteorol. 307, 108475 https://doi.org/10.1016/j.agrformet.2021.108475.
Zhou, J., Wei, C., Lai, Y., Wei, H., Tian, H., 2018. Application of the generalized clapeyron equation to freezing point depression and unfrozen water content. Water Resour. Res. 54, 9412–9431. https://doi.org/10.1029/2018WR023221.